

Control of Zonal DC Distribution Systems: A Stability Perspective

S.D. Sudhoff¹, S.F. Glover¹, S.H. Žak¹, S.D. Pekarek², E.J. Zivi³, D.E. Delisle⁴, J. Sauer⁴
¹Purdue University, ²University of Missouri-Rolla ³U.S. Naval Academy, ⁴Naval Surface Warfare Center

Abstract: Power electronics based DC distribution systems are attractive for finite inertia power systems such as those on ships and aircraft because of robustness and autonomy. However, they are also susceptible to negative impedance instabilities. In this work, two philosophies of system operation are considered. In the first approach, regulatory converters are designed to operate with perfect output regulation. In this approach, stability can be guaranteed provided that sufficient energy storage at each bus (electrolytic capacitance) is present. The second approach uses stabilizing feedback to modulate the converter output in response to its input thereby providing a means to ensure stability with greatly reduced energy storage. In this paper the relationship between stability, disturbance propagation, and energy storage is explored.

Key Words: system stability, zonal distribution, power electronics, disturbance propagation, energy storage

I. Introduction

Zonal dc distribution systems such as the one shown in Figure 1 are of a high degree of interest for robust mobile power systems. As such, they are currently the leading candidates for applications such as next generation warships and they have also been considered for aircraft. Figure 1 depicts a sample shipboard application. In this system, there are two power supplies (PS), one of which feeds the port bus, and the other feeds the starboard bus (only one connection is active at a time). There are three zones of dc distribution. Each zone is fed by a converter module (CM) operating from one of the two distribution busses. The converter modules feature a droop characteristic so that they normally share power. The three loads consist of an inverter module (IM) which in turn feeds an ac load, a motor controller (MC), and a generic constant power load (CPL).

The robustness in this system is achieved as follows. First, in the event that either a power supply fails, or a distribution bus is lost, then the other bus will pick up full system load without interruption in service. Faults between the converter module and diode are mitigated by imposing current limits on the converter modules; and again the bus opposite the fault can supply the component. Finally, faults within the components are mitigated through the converter module controls. The result is a highly robust system.

In this work, means used to ensure system stability are examined. The most straightforward approach is to utilize controls that perform their regulatory function without regard to input voltage. This results in an input admittance with a negative real part. However, in such a situation it can

be shown that stability can be insured provided that sufficient bus capacitance is present. One disadvantage of the bus capacitance is reduced power system power density caused by the additional weight and space requirements. A second disadvantage is that more energetic faults can occur which is undesirable from a damage control point of view.

As an alternative, the converter controls can be modified so as to allow disturbances in input voltage to affect the regulatory function. It will be shown that this can be used to greatly reduce the capacitive energy storage requirements, thereby increasing power density, as well as reducing the risk of fire during faults. The penalty is converter regulatory performance degradation.

Herein, a hybrid strategy is proposed for the system shown in Figure 1. A control strategy is examined wherein the endpoint loads - namely the IM, the MC, and the CPL, all perform their regulatory functions with complete disturbance rejection. However, the CM's use stabilizing feedback wherein perturbations of the converter module input voltages are allowed to propagate to the zonal loads.

The motivation of this approach is twofold. First, the power supplies are generally rectifier based and have relatively low control bandwidth and thus higher output impedance compared to the other converters. As a result, the port and starboard busses are more susceptible to stability problems than the zonal busses. At the zonal busses, it is observed that the converter modules have relatively high bandwidth and thus can be made to have low output impedance. Because of this low output impedance, the loads on the converter modules can be of the constant power variety without causing significant stability problems.

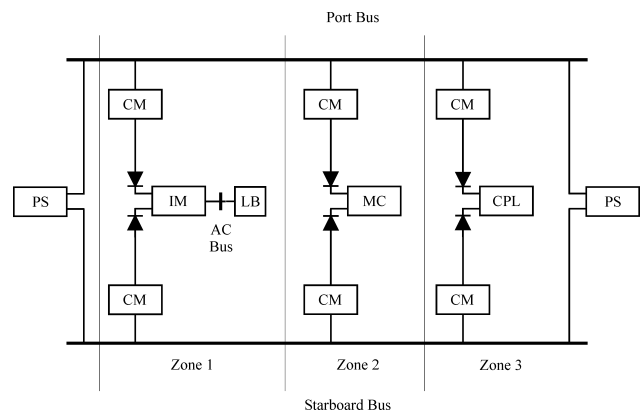


Figure 1. Zonal DC Distribution System.

II. End-Point Constant Power Load Consideration

In order to set the stage for this work, it is convenient to begin by considering the generic constant power load depicted in Figure 2. Therein, the load is modeled as an electrolytic capacitance C_l in parallel with an ideal constant power load where P_l is the power into the active portion of the converter.

Assuming that P_l is equal to the power required to achieve the desired regulatory function of the converter, P_l^* , the small signal input admittance of the constant power load may be readily expressed

$$\Delta i_l / \Delta v_l = C_l s - P_l^* / v_{l0}^2 \quad (1)$$

where s is the Laplace operator and v_{l0} is the nominal load converter input voltage. It is the second term that is problematic since it appears as a negative resistance, which has a highly destabilizing influence on the system.

In order to see how this affects system design, suppose that this load is fed from a simple source consisting of an ideal voltage v_s , with series resistance r_s , and series inductance L_s . Examination of the characteristic polynomial provides the following necessary and sufficient conditions for stability

$$r_s < v_{l0}^2 / P_l \quad (2)$$

and that

$$C_l v_{l0}^2 > P_l L_s / 2r_s \quad (3)$$

The first constraint (2) may be physically interpreted as a limitation on maximum power transfer. The second constraint (3) shows that the amount of capacitive energy storage goes up in direct proportion to the load power. In some cases this can require an extremely large amount of capacitance.

Previously, one method of mitigating the effects of this load is the nonlinear stabilizing control proposed in [1]. In this control, the power command is modulated as shown in Figure 3. As a result, it can be shown that the small signal input admittance looking into the load becomes

$$\Delta i_l / \Delta v_l = C_l s + P_l^* [n_{nsc}(1 - H_{nsc}(s)) - 1] / v_{l0}^2 \quad (4)$$

For frequencies in the pass band of H_{nsc} (which is a low pass filter) (4) reduces to

$$\Delta i_l / \Delta v_l = C_l s + P_l^* [n_{nsc} - 1] / v_{l0}^2 \quad (5)$$

III. One-Source Two-Bus System Consideration

In order to examine the relationship between control and power density from a system perspective, consider the one-source two-bus system depicted in Figure 4. This highly idealized system consists of a source, a converter module, and a load. Each of these elements is broken into two parts – a core converter (with no energy storage) and an electrolytic capacitance. This is done because the energy storage of a converter is dominated by the dc capacitance.

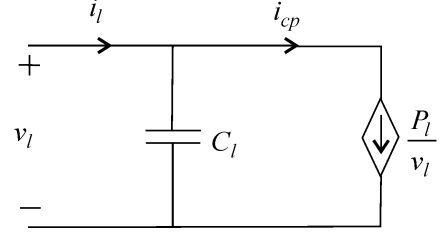


Figure 2. Constant Power Load.

In Figure 4, the linearized impedance of the core source converter is denoted S_c , the linearized H parameter of the

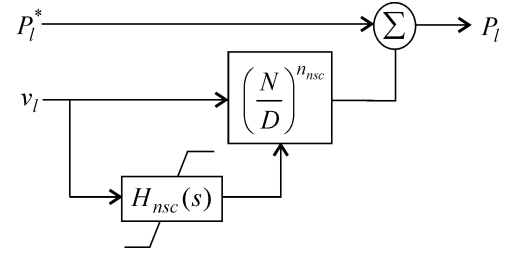


Figure 3. Nonlinear Stabilizing Control.

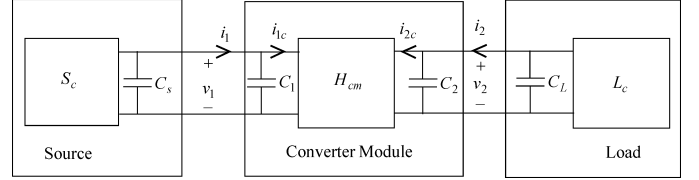


Figure 4. One-Source Two-Bus System.

core converter module is denoted H_{cm} , and the linearized load admittance of the core load converter is denoted L_c .

The converter module control architecture is shown in Figure 5. Therein $v_{cm,out0}^*$ is the nominal desired output voltage (in this case bus 2 voltage v_2), $v_{cm,out}^*$ is the instantaneous desired output voltage, $v_{cm,in}$ is the converter

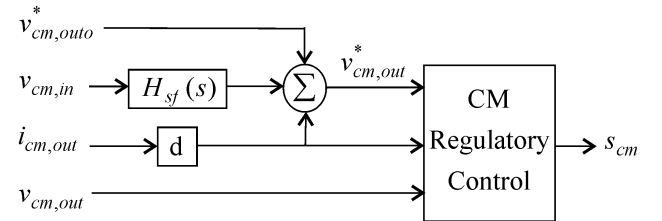


Figure 5. Generic Converter Module Control with Stabilizing Feedback.

module input voltage (in this case bus 1 voltage v_1), $i_{cm,out}$ is current into the output port of the converter module, and s_{cm} is a vector which describes the switching

states of each of the power electronic devices. The transfer function $H_{sf}(s)$ determines how much the input voltage is allowed to disturb the output voltage. This transfer function is selected to be a bandpass filter with passband gain K_{sf} . The d term is used to implement droop. The function of the regulatory control is to manipulate the switching of the power semiconductors such that the converter output voltage is as close as possible to $v_{cm,out}^*$.

It is interesting to examine the limiting case of what the impact on system performance would be if the output voltage is controlled with infinite bandwidth (perfectly regulated). Inserting the generic control shown in Figure 5 into the system shown in Figure 4 (thus $v_{cm,out} = v_2$ and $v_{cm,in} = v_1$) the bus 2 voltage would be described by

$$\Delta v_2 = H_{sf}(s)\Delta v_1 + d\Delta i_2 \quad (6)$$

Observe that if (6) is achieved and $H_{sf}(s)$ is stable then the stability at bus 2 is not an issue. The stability of bus 1, however, remains an issue. To this end, the small signal impedance looking into the converter module may be expressed

$$\frac{\Delta i_1}{\Delta v_1} = -\frac{i_{10}}{v_{10}} + C_1 s + H_{sf}(s) \frac{v_{20}}{v_{10}} \frac{C_2 s + L - \frac{i_{20}}{v_{20}}}{1 + Ld} \quad (7)$$

where L is the admittance looking into the load and the droop is set to $d = 0$. Assuming the load admittance is of the form

$$L = C_L s + L_c \quad (8)$$

where L_c is the admittance into the core of the load converter, (7) becomes

$$\frac{\Delta i_1}{\Delta v_1} = -\frac{i_{10}}{v_{10}} + C_1 s + H_{sf} \frac{v_{20}}{v_{10}} \left((C_2 + C_L) s + L_c - \frac{i_{20}}{v_{20}} \right) \quad (9)$$

If the core load is constant power,

$$L_c = i_{20}/v_{20} \quad (10)$$

Because of the polarity of the current reference, i_{20} is negative, and so the core admittance is a negative real number. Substitution of (10) into (9) yields

$$\frac{\Delta i_1}{\Delta v_1} = -\frac{i_{10}}{v_{10}} + C_1 s + H_{sf}(s) \frac{v_{20}}{v_{10}} (C_2 + C_L) s \quad (11)$$

From (11) several observations can be made. First, if there is no stabilizing feedback $H_{sf}(s) = 0$, then the converter module appears as a constant power load with shunt capacitance C_1 . However, if stabilizing feedback is present, then within the passband of $H_{sf}(s)$ (11) reduces to

$$\frac{\Delta i_1}{\Delta v_1} = -\frac{i_{10}}{v_{10}} + \left(C_1 + K_{sf} \frac{v_{20}}{v_{10}} (C_2 + C_L) \right) s \quad (12)$$

In this form, it can be seen that the admittance still has a negative real part. However, within the passband of K_{sf} the effective capacitance at the converter input is given by

$$C_{1,eff} = \left(C_1 + K_{sf} \frac{v_{20}}{v_{10}} (C_2 + C_L) \right) \quad (13)$$

The stabilizing feedback in this case does not impact the real part; however the input capacitance becomes and effective capacitance adjustable by the value of K_{sf} . Thereby allowing stability to be achieved with lower overall energy storage.

The details of this conclusion change somewhat if the characteristics of the load converter change. In particular, if the core load is resistive wherein

$$L_c = -i_{20}/v_{20} \quad (14)$$

Substitution of (14) into (7) and again setting $d = 0$ yields

$$\frac{\Delta i_1}{\Delta v_1} = -\frac{i_{10} + 2H_{sf}i_{20}}{v_{10}} + C_1 s + H_{sf} \frac{v_{20}}{v_{10}} (C_2 + C_L) s \quad (15)$$

which, within the passband of $H_{sf}(s)$, becomes

$$\frac{\Delta i_1}{\Delta v_1} = -\frac{i_{10} + 2K_{sf}i_{20}}{v_{10}} + C_{1,eff} s \quad (16)$$

where $C_{1,eff}$ is defined by (13). As can be seen, the capacitance looking into the converter module is again an effective capacitance. However, since i_{20} will be negative, by suitable choice of K_{sf} the real part of the admittance can be increased and even made positive improving system stability.

Based upon these observations consider a numerical study. The source is represented by a voltage $v_{s0} = 500$ V behind inductance $L_s = 18.7$ mH, and parasitic resistance $r_s = 2.46$ Ohms. These parameters correspond to a crude model of a 15 kW unregulated transformer rectifier power supply. This supply has a shunt output capacitance denoted C_s . The load converter consists of an input capacitance C_1 and a 5 kW constant power load. Finally, the converter module is assumed to be an ideal power converter with input capacitance C_1 , output capacitance C_2 and a nominal output voltage command of 420 V. For this study, the droop d is set to zero, and the stabilizer transfer function to

$$H_{sf}(s) = K_{sf} s \omega_2 / (s + \omega_1)(s + \omega_2) \quad (17)$$

where ω_1 and ω_2 are the beginning and end of the passband, set to $2\pi 0.1$ rad/s and $2\pi 500$ rad/s, respectively. The converter capacitances are set in accordance with

$$C_s = C_1 = C_{bus1}/2 \quad (18)$$

$$C_L = C_2 = C_{bus2}/2 \quad (19)$$

where C_{bus1} and C_{bus2} are the total installed capacitance at bus 1 and bus 2, respectively.

As stated, the focus of this study is to examine the relationship between total capacitive energy storage, disturbance propagation (as measured by K_{sf}) and, stability. The algorithm for this study is as follows. First, values for K_{sf} and C_{bus2} are assumed. Based upon these values, the value of capacitance at bus 1, C_{bus1} , required for

the system to be stable is calculated. This calculation is based on the closed loop characteristic polynomial of a source load system [2,3]

$$CLCP = 1 + SL \quad (20)$$

where S is the source impedance given by

$$S = (r + Ls) / ((r + Ls)Cs + 1) \quad (21)$$

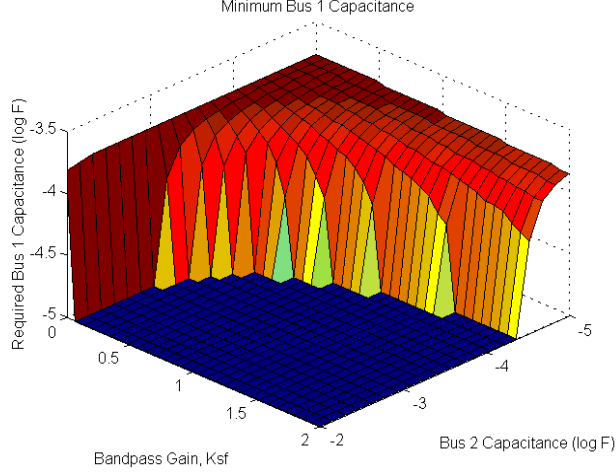


Figure 6 One-Source System Bus 1 Capacitance Versus Bus 2 Capacitance and Passband Stabilizing Gain.

and the L is the load admittance looking into the converter module which is set forth in (7).

$$E = \frac{1}{2} C_{bus1} v_{10}^2 + \frac{1}{2} C_{bus2} v_{20}^2 \quad (22)$$

In Figure 6, it can be observed that there is a large region for which no bus 1 capacitance is required. This region represents the ‘floor’ in Figure 6. Outside of this region, it can be seen that for any value of bus 2 capacitance, the amount of required bus 1 capacitance goes down with increasing K_{sf} .

The energy storage is depicted in Figure 7. Observe that the ‘floor’ in Figure 6, which is the region where C_{bus1} is fixed to its minimum value because it is not required for stability corresponds to the planar region in Figure 7. Further observe that there is a valley where this plane meets the curved portion of the characteristic. It is interesting to

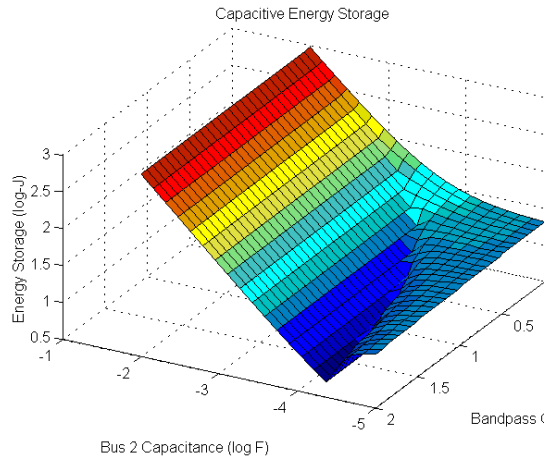


Figure 7. One-Source Energy Storage Versus Bus 2 Capacitance and Passband Stabilizing Gain.

note that for any value of K_{sf} there is a value of bus 2 capacitance that minimizes overall energy storage; furthermore this minimum value decreases as K_{sf} increases.

IV. Two-Source Three-Bus System Consideration

The next step in the development is to consider a single zone of a dc zonal power distribution system as depicted in Figure 8. Notation and definitions are similar to the previously considered system with the exception that an additional ‘p’ or ‘s’ is added as appropriate to designate port and starboard busses. In this system, the port and starboard converters attempt to regulate the load bus voltage in accordance with

$$\Delta v_2 = H_{sf}(s) \Delta v_{1p} + d \Delta i_{2p} \quad (23)$$

and

$$\Delta v_2 = H_{sf}(s) \Delta v_{1s} + d \Delta i_{2s} \quad (24)$$

respectively. From the load dynamics

$$-\Delta i_{2p} - \Delta i_{2s} = L(s) \Delta v_2 \quad (25)$$

Solving (26-28) yields

$$\Delta v_2 = H_{sf}(s) (\Delta v_{1p} + \Delta v_{1s}) / (2 + Ld) \quad (26)$$

Using power balance in conjunction with (26), the small –signal current perturbation into the port and starboard converters may be expressed in terms of wye-parameters as

$$\begin{bmatrix} \Delta i_{1p} \\ \Delta i_{1s} \end{bmatrix} = \begin{bmatrix} Y_{11}(s) & Y_{12}(s) \\ Y_{21}(s) & Y_{22}(s) \end{bmatrix} \begin{bmatrix} \Delta v_{1p} \\ \Delta v_{1s} \end{bmatrix} \quad (27)$$

where

$$Y_{11} = -\frac{i_{1p0}}{v_{1p0}} + sC_1 + H_{sf} \frac{v_{20}}{v_{1p0}} \frac{C_2 s + L - \frac{i_{2p0}}{v_{20}} + \frac{1}{d}}{2 + dL} \quad (28)$$

$$Y_{12} = H_{sf} \frac{v_{20}}{v_{1p0}} \frac{C_2 s - \frac{i_{2p0}}{v_{20}} - \frac{1}{d}}{2 + dL} \quad (29)$$

$$Y_{21} = H_{sf} \frac{v_{20}}{v_{1s0}} \frac{C_2 s - \frac{i_{2s0}}{v_{20}} - \frac{1}{d}}{2 + dL} \quad (30)$$

$$Y_{22} = -\frac{i_{1s0}}{v_{1s0}} + sC_1 + H_{sf} \frac{v_{20}}{v_{1s0}} \frac{C_2 s + L - \frac{i_{2s0}}{v_{20}} + \frac{1}{d}}{2 + dL} \quad (31)$$

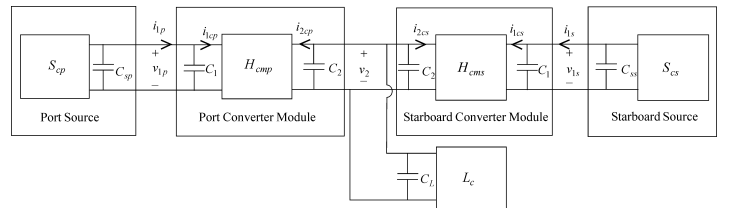


Figure 8 Single-Zone System.

In this case, it is quite difficult to see anything directly from the input admittance. However, for the sake of examining stability, note that the closed loop characteristic polynomial is readily expressed

$$CLCP = 1 + S_p Y_{11} + S_s Y_{22} + S_p S_s (Y_{11} Y_{22} - Y_{12} Y_{21}) \quad (32)$$

In order to gain insight into the relationship between required energy storage, disturbance rejection (again through K_{sf}), and stability, a study similar to the one in the previous section is conducted. The source, load, and converter module used in this study will all be identical to those of the previous study with the exception that droop is utilized ($d = 1$ Ohms), that the bus capacitance is now set in accordance with

$$C_{sp} = C_{ss} = C_1 = C_{bus1}/2 \quad (33)$$

$$C_2 = C_l = C_{bus2}/3 \quad (34)$$

and the system energy storage becomes

$$E = (C_{bus1} v_{1p0}^2 + C_{bus1} v_{2p0}^2 + C_{bus2} v_{2p0}^2) / 2 \quad (35)$$

In order to gauge the effect of stability on the zonal power system, the following study is conducted. For a given value of K_{sf} and C_{bus2} , the value of capacitance required for C_{bus1} is determined (by inspection of (32)). The resulting value of C_{bus1} and E are depicted in Figure 9 and 10.

In Figure 9, it can be seen that for a relatively large region, the required bus 1 capacitance decreases as either the bus 2 capacitances or disturbance bandpass gain K_{sf} increases. There is a region, however, where the required bus 1 capacitance is essentially zero. Unlike the previous study, note that counter intuitively, once in this region further increase in K_{sf} can actually result in an increased requirement on bus 1 capacitance.

Figure 10 depicts the total energy storage. Minimization of the capacitive energy storage favors larger values of K_{sf} and small values of bus 2 capacitance. However, there is also a local minima in the region of a bus 2 capacitance of 1 mF and K_{sf} of -20 dB which corresponds to the

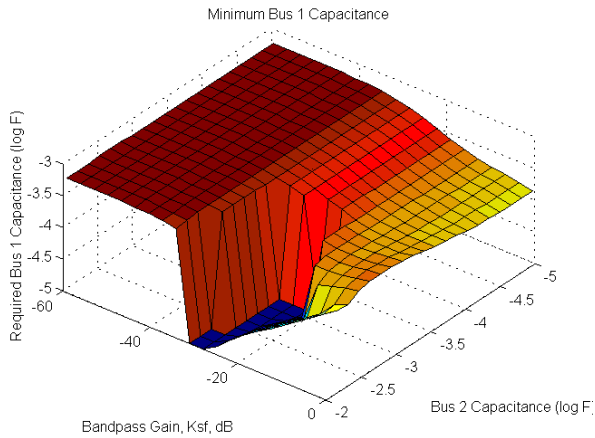


Figure 9. Single Zone System Bus 1 Capacitance Versus Bus 2 Capacitance and Passband Stabilizing Gain.

depressed region in Figure 9. The important conclusion in all of this is that by allowing a disturbance to propagate from the input of the converter modules to the output, the overall system energy storage can be reduced.

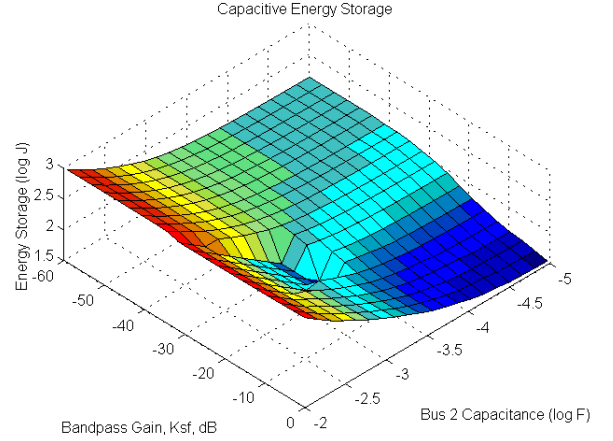


Figure 10. Single Zone System Energy Storage Versus Bus 2 Capacitance and Passband Stabilizing Gain.

V. System Application

In the previous two examples, the systems studied have been small and highly idealized. In this section it is shown, for the system in Figure 1, that stability can be achieved with reduced energy storage if an appropriate level of stabilizing feedback is used.

The first step in doing this is to view the component models as generalized quantities as described in [2,3] rather than simple impedances or admittances. In this way, uncertainty and the effects of multiple operating points can be addressed. Secondly, instead of simply insuring stability, the requirement will be that the system satisfies the ESAC stability criteria [2,3] with a 3 dB gain margin and a 30 degree phase margin.

The power supply considered is based on a transformer – dc link – rectifier. The ac source for this power supply is considered to be ideal source with a voltage of 560 V l-l rms ($\pm 5\%$) and the frequency of 60 Hz ($\pm 5\%$). The transformer has a turns ratio (primary to secondary) of 1.51, and a total leakage inductance (viewed from the primary side) of 2.08 to 4.16 mH. The dc link inductance and resistance associated with this inductance are 3.5 mH and 330 m Ω , respectively. Finally, the nominal output capacitance is 0.5 mF.

The converter model is based on the switch-average value model of the converter shown in Figure 11. Parameter values are: $r_{lin} = 0 \Omega$, $L_{in} = 0$ H, $r_{cin} = 0.4 \Omega$, $C_{in} = 476 \mu\text{F}$, $r_{lout} = 0.1 \Omega$, $L_{out} = XX$ H, $r_{cout} = 0.4 \Omega$, and $C_{out} = 476 \mu\text{F}$.

The converter control is depicted in Figure 12, which includes stabilizing feedback. Parameters for the control are: $\tau_{invc} = 1 \mu\text{s}$, $\tau_{invout} = 1 \mu\text{s}$, $\tau_{iniout} = 1 \mu\text{s}$, $d = 1$, $K_{pv} = 0.628$ A/V, $K_{iv} = 197.0$ As/V, $K_{sf} = 0.1$,

$\tau_{sf1} = 20$ ms, $\tau_{sf2} = 4$ ms, $K_{ii} = 15.7$ kA/s, $\Delta v_{outmax}^* = 20$ V, $i_{limit} = 20$ A, $i_{intlim} = 2$ A. The output of the control is a current command to a hysteretic controller.

The IM, MC, and CPL are all actually constant power in nature; for stability analysis these loads are treated as shown in Figure 2, where P_l is from 0 to 5 kW, and the input capacitance is 590 μ F with an effective series resistance of 0.127 Ω (which was included in the analysis).

The system is analyzed using the approach described in [2,3] using generalized impedances through the use of mapping operations to reduce the system to a single source load equivalent. Only the final portion of this analysis is included for brevity. In particular, the stability analysis of the port power supply as a source and the remainder of the system considered as a load is shown.

Figure 13 depicts the results from the stability analysis using the method of [2,3] with the listed system parameter values with the exception that the stabilizing feedback bandwidth gain, K_{sf} , was set to zero. In this figure, the

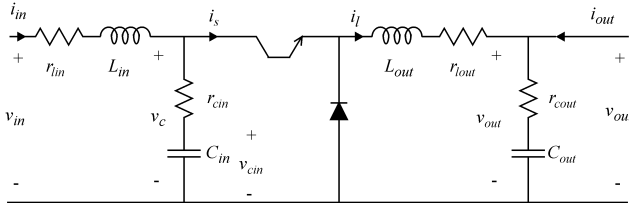


Figure 11. Converter Module.

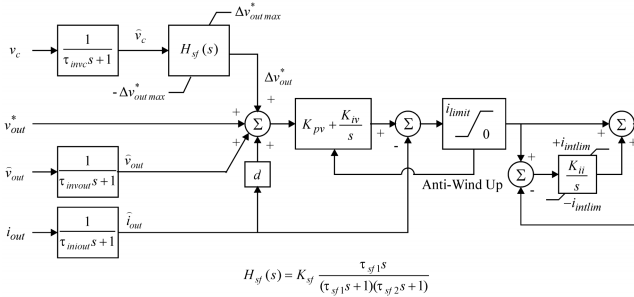


Figure 12. Converter Module Control

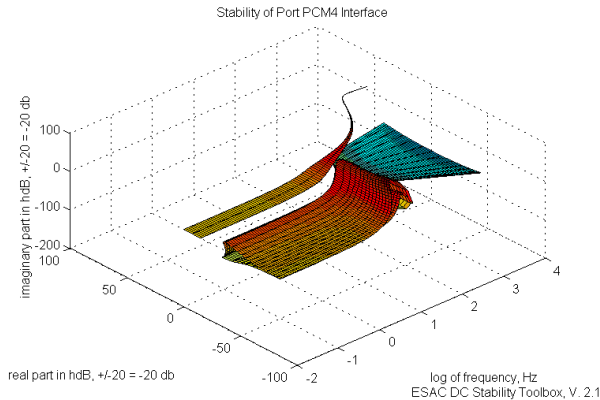


Figure 13. Stability of Port PS – System Interface with Full Capacitance and $K_{sf}=0$.

x-axis is log of frequency, and the y- and z- axis are real and imaginary part of admittance, in hybrid coordinates. In particular, in this coordinate system, complex numbers with a magnitude of less than -20 dB are represented on a linear scale with a constant of proportionality such that a magnitude of -20 dB corresponds to a mapped magnitude of 20; complex numbers with a magnitude greater than -20 dB are represented in dB offset such that -20 dB maps to 20; and the sign of the real and imaginary parts are the same in hybrid coordinates as their real and imaginary parts. The advantage of hybrid coordinates is that it avoids problems associated with wind up in phase.

The region to the right in this figure is the constraint on the total system load admittance placed on the port power supply calculated using [2,3]; the volume to the left is the generalized load admittance looking into the system. Since the two volumes do not intersect, the system is guaranteed to be stable at all operating points of interest.

The impact of reducing the power supply capacitance is depicted in Figure 14. In particular, the same study as shown in Figure 13 is repeated with the exception that the source capacitance is reduced from 1.5 mF to 0.5 mF. As seen in Figure 14, the system no longer satisfies the stability criteria. As a side note, the system also failed one of the sub-analysis (involving the starboard power supply).

In Figure 15, the reduced capacitance system is again considered. However, in this case, the stabilizing gain

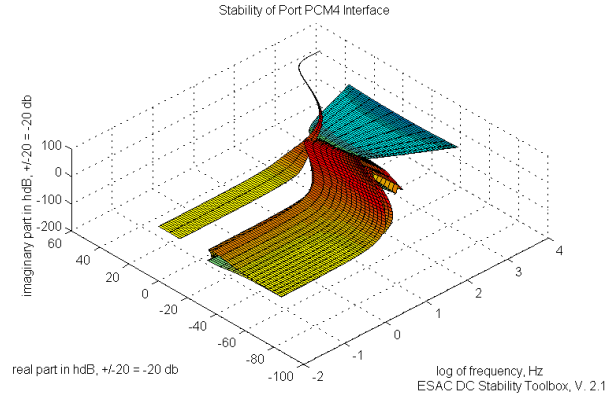


Figure 14. Stability of Port PS – System Interface With Reduced System Capacitance and $K_{sf}=0$.

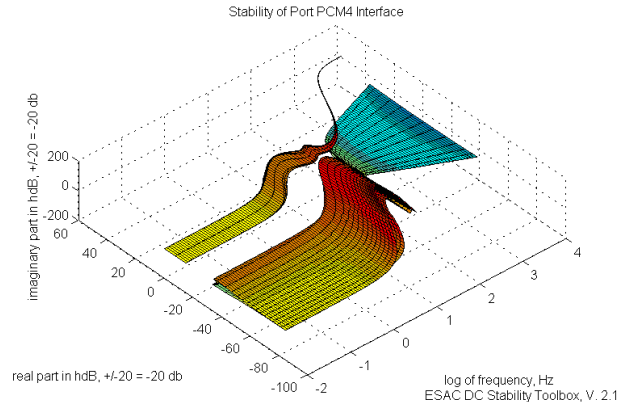


Figure 15. Stability of Port PS – System Interface With Reduced System Capacitance and $K_{sf}=0$.

K_{sf} has been set to 0.1. As can be seen, this substantially modifies the system load admittance within the bandpass of the stabilizing filter; allowing the stability criterion to be satisfied – and thereby demonstrating how allowing input voltage disturbances to propagate to the converter module output, system stability can be achieved with less energy storage.

VI. Conclusion

The chief result shown in this work is that a good strategy for achieving stability with minimal energy storage, and essentially no effect on the final regulatory function in dc zonal distribution systems is to carefully tailor the amount of disturbance propagation that occurs from the converter module input to the converter module output. Further reduction in energy storage requirements could possibly be achieved by allowing disturbance propagation from load inputs to the final regulatory function; but this could be undesirable for many applications. Further work needs to be done on exploring the control in the time

domain in order to insure the proposed control has attractive transient performance.

VI. References

- [1] S.D. Sudhoff, K.A. Corzine, S.F. Glover, H.J. Hegner, and H.N. Robey, "DC Link Stabilized Field Oriented Control of Electric Propulsion Systems," *IEEE Transactions on Energy Conversion*, Vol. 13, No. 1, March 1998.
- [2] S.D. Sudhoff, S.F. Glover, "Three Dimensional Stability Analysis of DC Power Electronics Based Systems," Proceedings of the Power Electronics Specialist Conference, Galway, Ireland, June 19-22, 2000, pp. 101-106.
- [3] S.D. Sudhoff, S.F. Glover, P.T. Lamm, D.H. Schmucker, D.E. Delisle, "Stability Analysis of DC Power Electronics Based Distribution Systems Using Admittance Space Constraints," *IEEE Transactions on Aerospace and Electronics Systems*, Vol. 36, No. 3, July 2000, pp. 965-973.